Relative importance of tropical SST anomalies in forcing East Asian summer monsoon circulation

Lei Fan,[1] Sang-Ik Shin,[2] Qinyu Liu,[1] and Zhengyu Liu[3,4]

Received 13 March 2013; revised 19 April 2013; accepted 19 April 2013; published 31 May 2013.

[1] The relative importance of tropical SST anomalies to the dominant variability of East Asian Summer Monsoon (EASM) circulation is investigated using an atmospheric general circulation model and a linear inverse model. It is found that the cooling over the central tropical Pacific is crucial in developing and maintaining the summertime northwest Pacific anticyclones, associated with the EASM precipitation. In this regard, the previously suggested El Niño event in the preceding winter and accompanying tropical Indian Ocean warming alone may not be enough to predict the strength of EASM circulation. Instead, monitoring and predicting the evolution of sea surface temperature anomalies in the central tropical Pacific, especially in spring to summer, may greatly improve the prediction of EASM circulation. **Citation:** Fan, L., S.-I. Shin, Q. Liu, and Z. Liu (2013), Relative importance of tropical SST anomalies in forcing East Asian summer monsoon circulation, *Geophys. Res. Lett.*, *40*, 2471–2477, doi:10.1002/grl.50494.

1. Background

[2] East Asian Summer Monsoon (EASM) has tremendous socio-economic impacts over one of the most populated regions encompassing China, Korea, and Japan, since the subtropical monsoon front known as Meiyu in China, referred to as Changma in Korea and Baiu in Japan, forms a primary driver of regional hydrological cycle [*Ding and Chan*, 2005] and the rivers especially in parallel with intense monsoonal rain band can cause devastating floods and droughts [*Jiang et al*., 2008].

[3] It is now well recognized that the dominant mode of the interannual variability of the EASM lower-tropospheric circulation is an anticyclonic/cyclonic anomaly over the northwestern Pacific, known as the northwestern Pacific anticyclone (WPAC)/cyclone (WPC) [*Wang et al*., 2008]. The WPAC anomaly and accompanying precipitation anomalies over China are shown in Figure 1: the leading empirical orthogonal function (EOF) of boreal summertime (June, July, and August; JJA. All the seasons in this paper are pointed to boreal season) 850 hPa winds and its correlation with sea-level pressure (SLP) and precipitation over China. The precipitation data used are the observed monthly station records from 1951 to 2010 compiled by the Beijing Climate Center (available at http://cmdp.ncc.cma.gov.cn). The 850 hPa winds and SLP data are National Centers for Environmental Prediction-National Center for Atmospheric Research (NCEP-NCAR) reanalysis [*Kalnay et al*., 1996] during the overlapping years. All the data sets have undergone a removal of long-term trend and interdecadal variability, since we focus on the interannual variability only. As expected, Figure 1 shows clear association between the WPAC anomaly and precipitation over the subtropical monsoon frontal region, the Yangtze-Huai River Valley (YHRV). It indicates a strengthened subtropical high and thereby intensified 850 hPa anticyclonic winds that enhance the moisture transport from the western tropical Pacific to the subtropical frontal region, and increase the rainfall over the YHRV region as indicated by high correlation coefficients of above 0.5 in Figure 1a. The area averaged time history of YHRV precipitation also matches well with the principle component (PC) of the first EOF mode (Figure 1b) indicating that the major floods are indeed associated with the anomalous WPAC.

[4] Previously, it was suggested that the summer WPAC anomaly is an extension of a preexisting anticyclone. It develops during the fall before the peak of El Niño and reaches its mature stage in late winter to early spring. It is pointed that this anticyclone can sustain into summer possibly through a local positive feedback over the western tropical Pacific between the atmospheric Rossby waves and the underlying SST anomalies (SSTA) in the presence of mean northeasterly trade winds [*Wang et al*., 2000; *Wang and Zhang*, 2002]. Another plausible sustaining mechanism is through the "capacitor effect" of the tropical Indian Ocean [TI; *Yang et al*., 2007; *Xie et al*., 2009]. In this mechanism, the TI warms up after the peak of El Niño through various atmospheric and oceanic teleconnections [*Liu and Alexander*, 2007], maintains these anomalies from spring to following summer, and then impacts to maintain the WPAC anomaly in summer.

[5] However, not all the observed summer WPACs, and thereby the major floods in the YHRV, are associated with the preceding El Niño events and accompanying TI warming. For instance, some El Niño events such as 1957/1958 and 1986/1987 are not followed by an anomalous summer WPAC. Moreover, in the summer of 1954 when the most devastating flood occurred in the YHRV, the anomalous WPAC was not accompanied with TI warming but rather cooling as a consequence of developing La Niña. *Lau and Nath* [2006] noticed that the warming (cooling)

Additional supporting information may be found in the online version of this article.

[1]Key Laboratory of Physical Oceanography, Ocean University of China, Qingdao, China.
[2]College of Marine Science, University of South Florida, St. Petersburg, Florida, USA.
[3]Laboratory of Climate, Ocean and Atmospheric Studies, Peking University, Beijing, China.
[4]Department of Atmospheric and Oceanic Sciences, University of Wisconsin-Madison, Madison, Wisconsin, USA.

Corresponding author: L. Fan, Key Laboratory of Physical Oceanography, Ocean University of China, Qingdao 266100, China. (leifan321@gmail.com)

0094-8276/13/10.1002/grl.50494

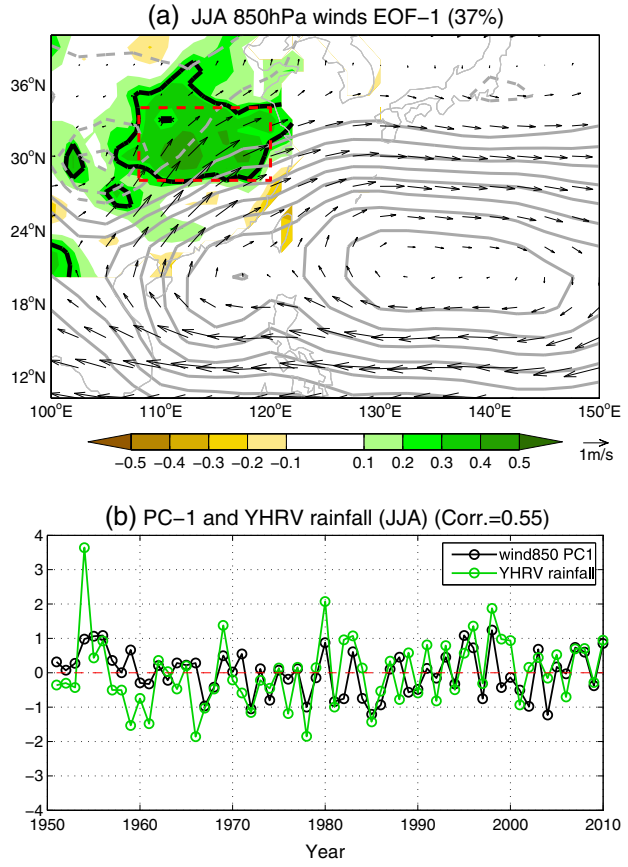

Figure 1. (a) The first EOF of summertime (JJA) 850 hPa winds (vectors) and (b) the accompanying PC-1 (black solid-open circle line). The correlation values between China precipitation and PC-1 are shown in Figure 1a as green shadings with black contour denoting the critical value at 95% confidence level (r = 0.26). The regression of sea level pressure on PC-1 is also shown in Figure 1a as gray contours with the interval 0.1 hPa. Solid lines are for positive values and dashed for negative; zero lines are omitted. In Figure 1b, the time series of YHRV rainfall anomalies spatially averaged over the red dashed box in Figure 1a is denoted as green solid-open circle line. The correlation between the PC-1 and YHRV rainfall time series is 0.55.

over the central tropical Pacific during the developing phase of El Niño can generate a cyclone (anticyclone) in boreal summer. Then, in which tropical ocean regions are SSTAs most critical in forcing the summer WPAC anomaly?

[6] This leads us to revisit the sensitivity of the WPAC anomaly to the pattern and timing of the tropical SSTAs. In this paper, we begin with an assessment of the sensitivity of summer WPAC anomaly to tropical SSTAs in section 2 based on a series of atmospheric general circulation model (GCM) simulations using a Max Planck Institute for Meteorology (MPIM) atmospheric GCM, the European Centre/Hamburg 5 (ECHAM5) [*Roeckner et al*., 2006]. In section 3, a Linear Inverse Model (LIM) [*Penland and Sardeshmukh*, 1995] will be used to examine the seasonal dependence of tropical SSTAs' impacts on the formation and maintenance of the WPAC anomaly. An observed composite analysis will be performed in section 4, and then summary and discussion will be given in section 5.

2. Sensitivity of the Summer WPAC Anomaly to Tropical SST Anomalies

[7] The ECHAM 5 performance in simulating the WPAC anomaly and related land precipitation pattern is validated in Figure S1 in the auxiliary material by comparing the combined (multi-variable) EOF-1 of SLP, 850 hPa winds, and land precipitation (Global Precipitation Climatology Project) between the observation and 24 ECHAM5 ensemble mean (each are initialized with different atmospheric conditions). The two results show considerable consistency either in the spatial pattern or the time series (with correlation up to 0.64) except for the slightly shifted China maximum rainfall center, indicating the realistic simulation of ECHAM 5 for the EASM circulation.

[8] To derive the sensitivity map of the summer WPAC anomaly to the tropical SSTAs, we analyzed a series of atmospheric GCM simulations. In these simulations, which have a horizontal resolution of T42 (~2.8° in longitude and latitude), a hypothetical cosine squared shape patch of SSTAs was prescribed on top of the climatological annual cycle over the 43 different tropical locations (see Figure 2a). For each patch location, 20 ensemble members of warm and 20 ensemble members of cold patch experiments were performed for a 25 month duration starting from October. Then, the linear WPAC response to SSTAs over each patch during JJA was estimated as $\mathrm{WPAC}^{\mathrm{linear}} = (\mathrm{WPAC}^{\mathrm{warm}} - \mathrm{WPAC}^{\mathrm{cold}})/2$, where the WPAC is defined as the 850 hPa zonal wind difference in two Western Pacific regions—the average in 20°N–30°N, 110°E–140°E minus that in 5°N–15°N, 90°E–130°E—as suggested by *Wang et al* [2008].

[9] To generate the meaningful sensitivity map, we followed the same procedures outlined by *Barsugli et al*. [2006] and *Shin et al*. [2010b]. First, the raw sensitivity values of WPAC to each patch forcing were estimated. For the k-th patch whose SSTAs is given by T_{kj} on the T42 model grid j, the raw sensitivity s_k is

$$s_k = \frac{\mathrm{WPAC}_k^{\mathrm{linear}}}{\sum_j T_{kj} A_j},$$

where A_j is the area elements for the j-th grid point associated with patch k. The estimated sensitivity values were assigned to the geographical centers of the patches, and then spatially smoothed using the smoothing spline procedure [*Gu*, 1989] based on the signal-to-noise ratio. This map can also be viewed as the optimal SSTA forcing pattern (T_{OPT}) for WPAC when normalized by an RMS (root mean square) amplitude over the tropics—a hypothetical SSTA forcing pattern that can maximize the anomalous WPAC response (The normalized optimal SSTA pattern is $T_{\mathrm{OPT}} = s_A \left(\frac{1}{A_p} \int_p s_A^2 \, \mathrm{d}A \right)^{-1/2}$, where s_{A} is the smoothed sensitivity values for the WPAC, and A_p is the area spanned by the patches.). We further scaled the sensitivity map with the magnitudes of local SST variability by multiplying its standard deviation to take into account the extent to which the observed SSTs can vary.

[10] The patch derived sensitivity map is shown in Figure 2b along with the linearly reconstructed 850 hPa wind response to the normalized T_{OPT} (Formally, the patch experiments can be

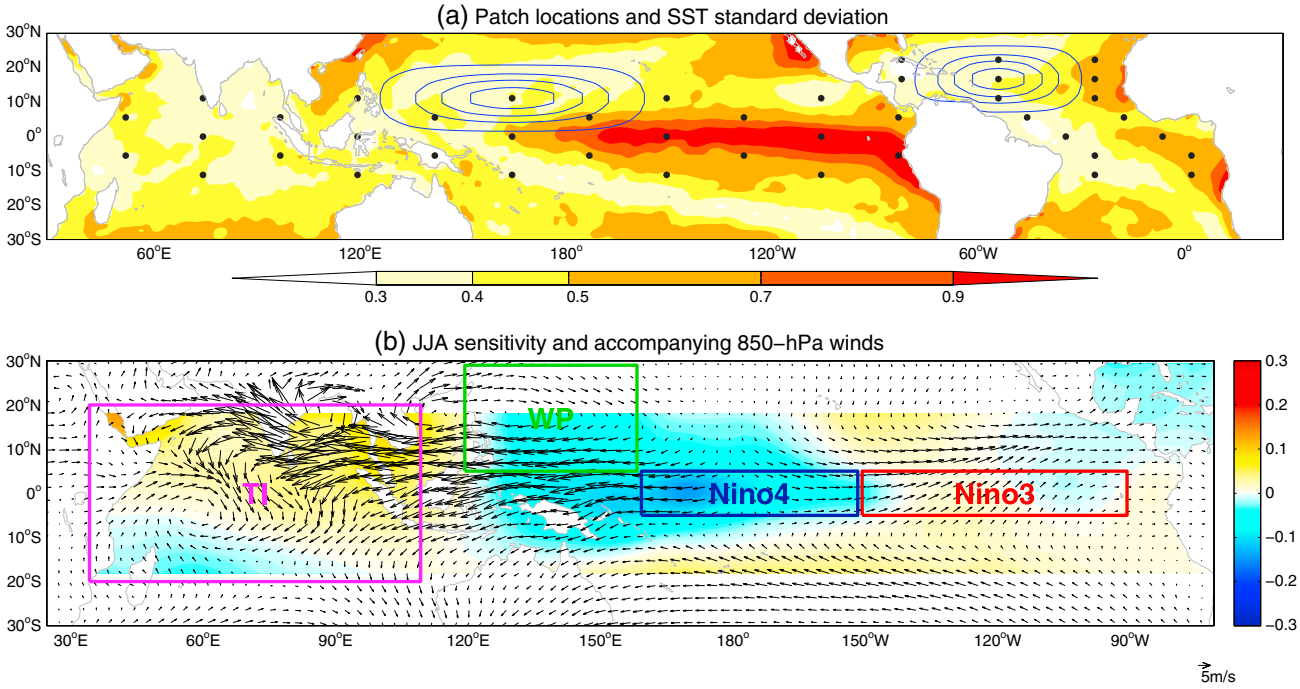

Figure 2. (a) Patch locations and summertime (JJA) SST standard deviation. The black dots denote the center of each patch and the blue contours in the Pacific and Atlantic are the examples of model forcing SST anomalies over the Indo-Pacific and Atlantic Oceans, respectively. The contours start from 0.1°C with the interval of 0.5°C. (b) The sensitivity map of summer (JJA) WPAC to the tropical SSTs (shading) scaled with SST standard deviation. The unit of the sensitivity map for the WPAC index is $\mathrm{m\,s^{-1}/[10^6\,km^2{}^\circ C]}$. The vectors are the linearly constructed 850 hPa wind responses to the optimal SST pattern. See text for details.

viewed as an application of "Fuzzy Green's function" to the climate science, based on the concept that the atmospheric responses to any tropical SSTA patterns can be approximately estimated as the sum of responses to small patches of SSTAs [*Barsugli and Sardeshmukh*, 2002.]). The reconstruction was done as the sum of responses of each patch weighted by T_{OPT} over that patch. It shows that the summer WPAC anomaly is sensitive to the east-west dipole pattern of cooling in the west-central tropical Pacific and warming in the TI. The eastern tropical Pacific, on the other hand, only plays a minor role. While the positive sensitivity of TI warming on the WPAC anomaly has already been highlighted in previous studies [*Xie et al.*, 2009], one may note that the cooling over the west-central tropical Pacific, approximately Niño-4 region, is noticeably instrumental in the summer WPAC formation and maintenance. This can be understood with tropical wave responses to surface diabatic heating [*Lau and Nath*, 2006]. The central tropical Pacific cooling induces subsidence Rossby waves [*Matsuno*, 1966; *Gill*, 1980]. This mechanism is presented in Figure S2 by showing atmospheric anomalies as responses to a patch of cold SST anomalies in the central Pacific in JJA. The WPAC anomaly is evidently shown in Figure S2a. In this way, the cooling over the central Pacific plays a vital role in forming and maintaining the WPAC during summer.

[11] Considering the previous results that the eastern tropical Pacific (Niño-3) warming and the western Pacific cooling are essential in WPAC development in winter to early spring [*Wang and Zhang*, 2002] and the delayed warming over the TI is important in maintaining the WPAC in spring to summer [*Yang et al.*, 2007; *Xie et al.*, 2009], the role of Niño-4 cooling in summer provides another clue on how WPAC does maintain its strength up to the peak of the EASM rainy season. The relative importance of these oceanic areas in forcing the anticyclone in different seasons will be examined in the next section.

3. Seasonal Dependence of Tropical SSTA Impacts on WPAC Anomaly

[12] Based upon the sensitivity map in Figure 2b, we construct statistical models to assess the seasonal impacts of regional SSTAs on the formation and maintenance of the WPAC anomaly. To this end, we selected four key tropical ocean regions based on the sensitivity map. They are Niño-3 (5°S–5°N, 150°W–90°W), TI (20°S–20°N, 30°E–110°E), Niño-4 (5°S–5°N, 160°E–150°W), and the local western tropical Pacific Ocean (WP; 5°N–30°N, 120°E–160°E). The signs of Niño-4 and WP were reversed to highlight the impacts of cooling over both regions (see legend to Figure 3). For the WPAC index, we used the PC time series of monthly EOF-1 of 850 hPa winds to take into account the fact that the center of the WPAC changes from winter to summer (figure not shown).

[13] The simultaneous correlation coefficients between the WPAC anomaly and four SSTAs are shown in Figure 3a (Because of the persistency of SSTAs and anticyclone, correlations with lags of −1, 0, or 1 month show similar results.). The Niño-3 and TI, and WP cooling are both positively correlated with the WPAC in winter. As the season progresses, the correlation between Niño-3 and the WPAC decreases, while the correlation between the TI and WPAC remains significant until spring and then becomes

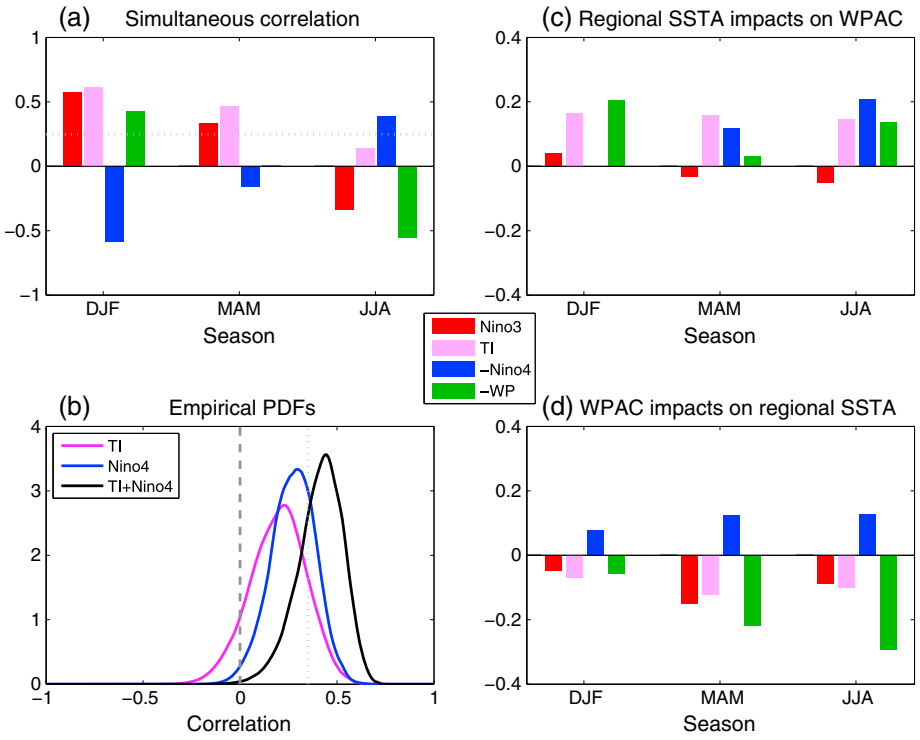

Figure 3. (a) The simultaneous correlation between the WPAC anomaly and SSTAs for each season. (b) The empirical PDF of the correlation values between the observed and regression model forecasted WPACs. See test for details. (c) The feedback coefficients derived from LIM indicating SSTAs impact on WPAC. (d) The same as Figure 3c, but for the coefficients indicating WPAC impact on SSTAs. The dotted lines in Figures 3a and 3b denote the critical correlation values at 95% confidence level for the sample size 63 and 32, respectively. To highlight the impact of Niño-4 cooling and WP cooling on the summer WPAC, the sign of both SSTA time series are reversed before computation.

insignificant in summer. For the WP, a cold WP is correlated with the WPAC in winter while the sign is reversed in summer. Noteworthy is that the Niño-4 cooling becomes a more significant remote forcing for the WPAC in boreal summer.

[14] It should be noted that the correlation analysis provides only the association of the processes, not the causality of the processes. In this regard, we further use LIM [*Penland and Sardeshmukh*, 1995] to separate the influence of atmosphere on SSTA from that of SSTA on atmosphere. Here, we only briefly introduce the LIM methodology, and interested readers can find more detailed information on the LIM in geographical space elsewhere [e.g., *Shin et al.* 2010a].

[15] Let us consider the coupled system consisting of the time series of the WPAC index A and 4-regional (Niño-3, TI, Niño-4, and WP) SSTAs given by T_1, T_2, T_3, and T_4, respectively. The evolution of the system can be represented as

$$\frac{d\mathbf{x}}{dt} = \mathbf{L}\mathbf{x} + \mathbf{B}\boldsymbol{\eta},$$

where $\mathbf{x} = (A \quad T_1 \quad T_2 \quad T_3 \quad T_4)^{\mathrm{T}}$ is the state vector, L is the deterministic linear feedback matrix, and $\mathbf{B}\boldsymbol{\eta}$ represents the stochastic forcings ($\mathbf{B}$ is a constant matrix and $\boldsymbol{\eta}$ is a white noise vector). The matrix L can be determined by an error variance minimization procedure as $\mathbf{L} = \tau_0^{-1} \ln\left[\mathbf{C}(\tau_0)\mathbf{C}(0)^{-1}\right]$, where $\mathbf{C}(\tau_0)$ and $\mathbf{C}(0)$ are the covariance matrix of $\mathbf{x}$ at the time lag τ_0 and 0, respectively. In this study, we estimate $\mathbf{L}$ for each season (DJF, MAM, and JJA) separately as previously done by *Liu et al.* [2012], and the results shown here are not sensitive to the choice of lag $\tau_0 = 1$ or 2 months.

[16] The linear feedback matrix $\mathbf{L}$ provides the comprehensive information on the mutual interactions, since its elements, L_{ij}, represent the impacts of the j-th element on the i-th one (Note that $L_{ij} \neq L_{ji}$). Here, the particular emphasis is given to the elements of the first row $L_{Aj}(j = 1, 2, 3, 4)$ that represents the impacts of the j-th SSTA forcing on the WPAC, and those of the first column L_{iA} $(i = 1,2,3,4)$ that represents the impacts of the WPAC on the i-th SSTA. The impacts of the four SSTAs on the WPAC are shown in Figure 3c, and the impacts of the WPAC on those SSTAs are shown in Figure 3d for different seasons.

[17] The positive L_{A4} (green bars) in Figure 3c in all seasons indicates that the local WP cooling intensifies the WPAC anomaly, especially in winter, while the negative L_{4A} in Figure 3d indicates that the WPAC induces (decrease) local WP warming (cooling), especially in summer. These opposite signs of L_{A4} and L_{4A} indicate a negative local WPAC-SST feedback probably by cloud-radiation mechanism. In summer (winter), the WPAC (WP) impact on the WP (WPAC) overwhelms that of WP (WPAC) on the WPAC (WP). Therefore, the summer positive correlation between the WPAC and WP warming SSTAs shown in Figure 3a is a mere reflection of atmospheric impacts on local SSTAs. In this regard, the local SSTA forcing on the WPAC shown in the atmospheric GCM sensitivity map (WP in Figure 2b) may not operate in the interannual time scales considered here. Note that the sensitivity map should not be interpreted as what is happening, instead it suggests a potential to happen. Thus, a local cooling and anticyclone relationship may still be justified, but simply it is not dominant in interannual time scales (The local

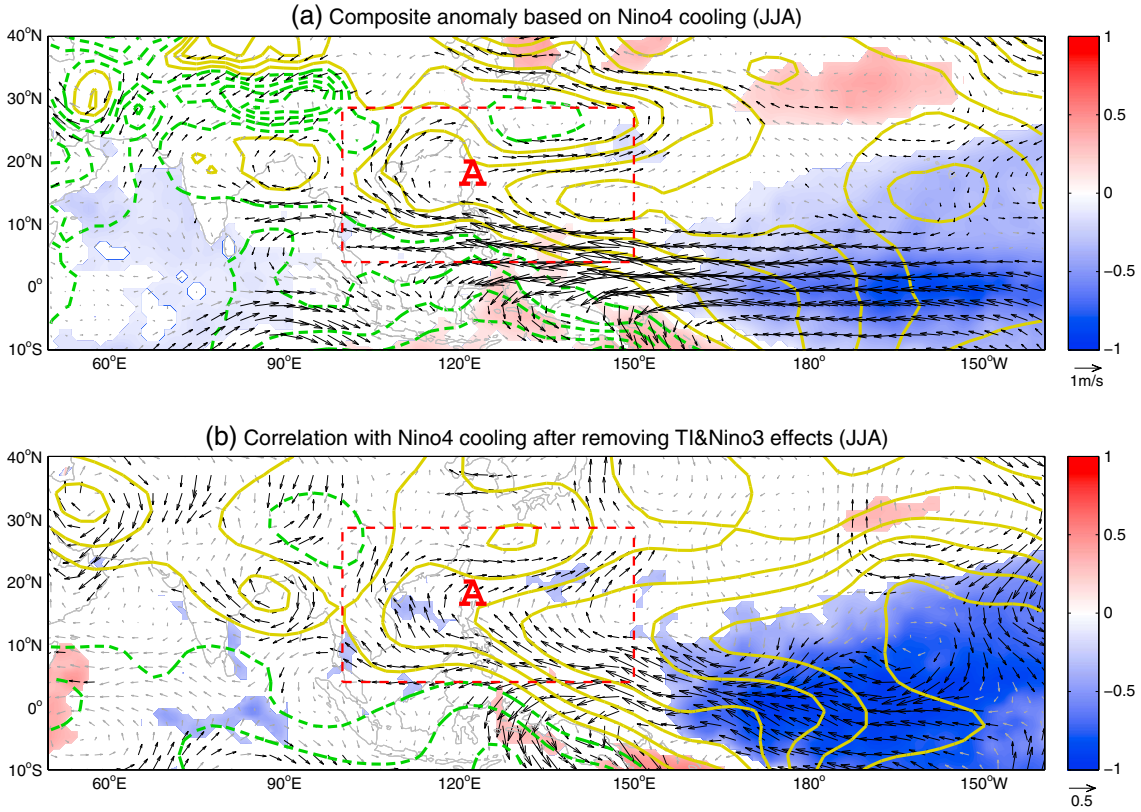

Figure 4. (a) Composite JJA anomalies based on Niño-4 cooling averaged over 19 years when the normalized JJA Niño-4 SSTA below 0.75 times of its standard deviation, namely, 1950, 1954,1955, 1956, 1964, 1971, 1973, 1974, 1975, 1976, 1984, 1985, 1988, 1989, 1998, 1999, 2000, 2008, and 2010. (b) Partial correlations with Niño-4 cooling controlling for the TI and Niño-3 SSTAs. 850 hPa winds (vectors), sea level pressure (contours with interval 0.1 hPa in Figure 4a and 0.1 in Figure 4b, green dashes are for negative and yellow solid for positive and zero values), and SSTA (shading) are shown. Significance tests from a two-tailed Student's *t* test at 90% confidence level are performed for SSTA and 850 hPa winds. For the SSTA, only significant values are shown; for the 850 hPa winds, significant vectors are denoted in black color while others in gray.

cooling-anticyclone relation may hold for the decadal or longer timescales. The correct estimation of the sign of atmosphere-ocean interactions over the WP brings us more confidence in assessing the results of impacts of other regional SSTAs on the WPAC. The local WP cooling exerts the largest impacts in winter, consistent with previous studies [*Wang et al.*, 2000], while the most instrumental region in spring is the TI warming (Figure 3c).

[18] Noteworthy is that in summer, the cooling in Niño-4 becomes the most important player. This result is in agreement with the correlation analysis shown in Figure 3a. Interestingly, the effect of the WPAC on Niño-4 SSTAs in summer is also positive (Figure 3d). It implies that a positive feedback operates between Niño-4 cooling and the WPAC anomaly. The plausible explanation is that a cooling over the Niño-4 region can induce the easterlies and anticyclone on its west and northwest flanks (Figure S2a), while the easterlies in the south of anticyclone in turn maintains the Niño-4 cooling by wind-thermocline mechanism known as one of the La Niña developing mechanisms [*Weisberg and Wang*, 1997]. In summary, both correlation and LIM results highlight the crucial importance of the Niño-4 cooling in the formation and maintenance of the WPAC in boreal summer. The TI influence does still persist in summer but it is weaker than that in spring.

[19] To further validate the robustness of the Niño-4 cooling contribution to the summer WPAC, we constructed and performed the regression models of the WPAC on, respectively, TI SSTAs alone, Niño-4 SSTAs alone, and SSTAs of both regions combined. We performed 10,000 predictions for each case by using 1 month lag, i.e., regressing the JJA-averaged WPAC index onto MJJ-averaged SSTAs. For each exercise, we randomly chose 31 years (training period) out of a 63 year record (1948–2010) to build the regression model, made a forecast for a 32 year time span (forecast period), and then computed the correlation between the actual and the forecasted WPAC indices to measure the potential forecast skills. The empirical probability density functions (PDFs) of these skills are shown in Figure 3b, which clearly shows that the potential forecast skills are improved substantially when we incorporated the Niño-4 SSTAs. This provides further evidence that the Niño-4 cooling is indeed critical for maintaining the summer WPAC anomaly.

4. Observed WPAC Response to Central Pacific Cooling in Boreal Summer

[20] In this section, we assess the observed WPAC response to the central Pacific cooling using composite and partial correlation analysis of the 850 hPa wind and SLP

derived from NCEP-NCAR reanalysis and SSTA from the Hadley Centre Sea Ice and Sea Surface Temperature data set [*Rayner et al*., 2003] during the years 1948–2010. Figure 4a shows the JJA composite results based on the Niño-4 cooling years (listed in the figure caption) regardless of the TI warming. Figure 4b shows the partial correlation with Niño-4 cooling by removing the TI and Niño-3 influences. Both panels clearly show the WPAC and accompanying positive SLP anomalies extending to the Western Pacific, similar to Figure S2. It is worth noting that the response pattern is obtained in the absence of TI warming.

[21] The SSTA pattern in Figure 4 is reminiscent of the developing La Niña. A detailed composite analysis for different El Niño-Southern Oscillation (ENSO) phases is shown in Figure S3 (see the years listed in Table S1), which also highlights the role of Niño-4 cooling or La Niña development (Figure S3h,k). Figure S3e indicates that without Niño-4 cooling, the WPAC anomaly can hardly sustain into summer during the El Niño decay. It suggests that the commonly known relationship between El Niño decay and summer WPAC anomaly may be fragile, unless the La Niña-like condition is developing over the central tropical Pacific. However, because of the asymmetry of ENSO duration [*Okumura et al*., 2011], the years in which the strongest El Niños decay tend to be La Niña developing years (like 1998, 1983, 1973, and 2010). That may be the cause of the illusion that the summer WPAC anomaly was attributed to the preceding strong El Niño. We also found an asymmetry between the atmospheric anomalies related to the Central Pacific warming and cooling. The WPAC shown in Figure 4a is much stronger than its counterpart, the cyclone from a composite based on Niño-4 warming (Figure S4). *Okumura et al* [2011] pointed out that due to the nonlinear response of atmospheric convection to SST forcing, there is a westward displacement of rainfall anomalies during La Niña. Consequently, the surface wind responses over the Western Pacific are more dominated by Central-East Pacific SST during La Niña than that during El Niño. This mechanism provide a key to understand the asymmetry between Figure 4a and Figure S4.

5. Summary and Discussion

[22] Conventionally, the formation and maintenance of the boreal summer WPAC anomaly and accompanying floods in China were mainly attributed to the El Niño events in the preceding winter or accompanying TI warming in spring. In this study, based on the sensitivity map derived from MPIM ECHAM5 simulations, the remote and local feedbacks derived from LIM and the results from composite analyses, we presented the relative importance of SST over four key oceanic regions in forcing the WPAC, reaching the conclusion that the cooling over the central tropical Pacific is critical in developing and maintaining the summer WPAC anomaly. Thus, the summer WPAC and accompanying floods in China may not only be a residual effect of El Niño or delayed TI warming, but may also be a response to the cooling over the central tropical Pacific.

[23] As a general conclusion, the present results can suggest the influence of the El Niño (La Niña) Modoki [*Ashok et al*., 2007] events when the largest warm (cold) SST anomalies appear in the central Pacific. According to our results, boreal summer El Niño (La Niña) Modoki would promote the western Pacific cyclone (anticyclone) and bring negative (positive) summer rainfall anomalies over the subtropical monsoon front, the YHRV region of China. This is in agreement with previous studies [*Ashok et al*., 2007, Figure 9b; *Wang and Wang*, 2013, Figure 1]. The Niño-4 region represents the westernmost boundary of the central-eastern Pacific SSTA extension during El Niño (La Niña); therefore, for summer El Niño (La Niña) events with equatorial warm (cold) SST anomalies that extend more westward, like the El Niño Modoki II classified by *Wang and Wang* [2013], the Western Pacific cyclone (anticyclone) and deficient (abundant) YHRV rainfall are more likely to happen.

[24] Lastly, forecasting floods in China remains a formidable challenge and may involve many other factors that are not considered here. However, the current study suggests that, different from the previous ones, the El Niño event in the preceding winter and accompanying TI warming alone may not be enough to predict the strength of the EASM circulation and the flood in China. Instead, monitoring and predicting the evolution of SSTAs in the central tropical Pacific, especially in spring to summer, may greatly improve such predictions.

[25] **Acknowledgments.** We thank Prof. Wang Bin for helpful discussions. We also thank two anonymous reviewers for their helpful and constructive comments. This work is supported by the National Basic Research Program of China (2012CB955602, 2012CB955200), Natural Science Foundation of China (41176006,40921004), Ministry of Science and Technology of China (GYHY200906016), and Korea National Institute of Meteorological Research (SS).

[26] The Editor thanks two anonymous reviewers for their assistance in evaluating this paper.

References

Ashok, K., S. K. Behera, S. A. Rao, H. Weng, and T. Yamagata (2007), El Niño Modoki and its possible teleconnection, *J. Geophys. Res.*, *112*, C11007, doi:10.1029/2006JC003798.

Barsugli, J. J., and P. D. Sardeshmukh (2002), Global atmospheric sensitivity to tropical SST anomalies throughout the Indo-Pacific basin, *J. Climate*, *15*, 3427–3442.

Barsugli, J. J., S.-I. Shin, and P. D. Sardeshmukh (2006), Sensitivity of global warming to the pattern of tropical ocean warming, *Clim. Dyn.*, *27*, 483–492.

Ding, Y., and J. C. L. Chan (2005), The East Asian summer monsoon: An overview, *Meteorol. Atmos. Phys.*, *89*, 117–142.

Gill, A. E. (1980), Some simple solutions for heat-induced tropical circulation, *Quart. J. Roy. Meteor. Soc.*, *106*, 447–462.

Gu, C. (1989), RKPACK and its applications: Fitting smoothing spline models, *Proc. Stat. Comp. Sec.*, *Amer. Stat. Soc.*, 42–51.

Jiang, T., Z. W. Kundzewicz, and B. Su (2008), Changes in monthly precipitation and flood hazard in the Yangtze River Basin, China, *Int. J. Climatol*, *28*, 1471–1481.

Kalnay, et al. (1996), The NCEP/NCAR 40-year reanalysis project, *Bull. Amer. Meteor. Soc.*, *77*, 437–470.

Lau, N.-C., and M. J. Nath (2006), ENSO modulation of the interannual and intraseasonal variability of the East Asian Monsoon—A model study, *J. Climate*, *19*, 4508–4530.

Liu, Z., and M. A. Alexander (2007), Atmospheric bridge, oceanic tunnel and global climatic teleconnections, *Rev. of Geophys.*, *45*, RG2005, doi:10.1029/2005RG000172.

Liu, Z., L. Fan, S.-I. Shin, and Q. Liu (2012), Assessing atmospheric response to surface forcing in the observations. Part II: Cross validation of seasonal response using GEFA and LIM, *J. Climate*, *25*, 6817–6834.

Matsuno, T. (1966), Quasi-geostrophic motions in equatorial areas, *J. Meteorol. Soc. Jpn.*, *2*, 25–43.

Okumura, Y. M., M. Ohba, C. Deser, and H. Ueda (2011), A proposed mechanism for the asymmetric duration of El Niño and La Niña, *J. Climate*, *24*, 3822–3829.

Penland, C., and P. D. Sardeshmukh (1995), The optimal growth of tropical sea surface temperature anomalies, *J. Climate*, *8*, 1999–2024.

Rayner, N. A., E. C. Kent, and A. Kaplan (2003), Global analyses of sea surface temperature, sea ice, and night marine air temperature since the late nineteenth century, *J. Geophys. Res.*, *108*(D14), 4407, doi:10.1029/2002_JD002670.

Roeckner, E., et al. (2006), Sensitivity of simulated climate to horizontal and vertical resolution in the ECHAM5 atmosphere model, *J. Climate*, *19*, 3771–3791.

Shin, S.-I., P. D. Sardeshmukh, and K. Pegion (2010a), Realism of local and remote feedbacks on tropical sea surface temperatures in climate models. *J. Geophys. Res.*, *115*, D21110, doi:10.1029/2010JD013927.

Shin, S.-I., P. D. Sardeshmukh, and R. S. Webb (2010b), Optimal tropical temperature forcing of North American drought, *J. Climate*, *23*, 3907–3917.

Wang, B., R. Wu, and X. Fu (2000), Pacific–East Asian teleconnection: How does ENSO affect East Asian climate?, *J. Climate*, *13*, 1517–1536.

Wang, B., and Q. Zhang (2002), Pacific–East Asian teleconnection. Part II: How the Philippine Sea anomalous anticyclone is established during El Niño development, *J. Climate*, *15*, 3252–3265.

Wang, B., Z. Wu, J. Li, J. Liu, C.-P. Chang, Y. Ding, and G. Wu (2008), How to measure the strength of the East Asian Summer Monsoon, *J. Climate*, *21*, 4449–4463.

Wang, C., and X. Wang (2013), Classifying El Niño Modoki I and II by different impacts on rainfall in Southern China and typhoon tracks, *J. Climate*, *26*, 1322–1338.

Weisberg, R. H., and C. Wang (1997), A western Pacific oscillator paradigm for the El Niño-Southern Oscillation, *Geophys. Res. Lett.*, *24*, 779–782.

Xie, S.-P., K. Hu, J. Hafner, H. Tokinaga, Y. Du, G. Huang, and T. Sampe (2009), Indian Ocean capacitor effect on Indo–Western Pacific climate during the summer following El Niño, *J. Climate*, *22*, 730–747.

Yang, J., Q. Liu, S.-P. Xie, Z. Liu, and L. Wu (2007), Impact of the Indian Ocean SST basin mode on the Asian summer monsoon, *Geophys. Res. Lett.*, *34*, L02708, doi:10.1029/2006GL028571.